A Model-Predictive Hierarchical-Control Framework for Aggregating Residential DERs to Provide Grid Regulation Services

Preprint

Kumar Utkarsh, Fei Ding, Changhong Zhao, Harsha Padullaparti, and Xin Jin

National Renewable Energy Laboratory

Presented at the 2020 IEEE Conference on Innovative Smart Grid Technologies (IEEE ISGT)
Washington, D.C.
February 17–20, 2020

Conference Paper
NREL/CP-5D00-74827
February 2020

A Model-Predictive Hierarchical-Control Framework for Aggregating Residential DERs to Provide Grid Regulation Services

Preprint

Kumar Utkarsh, Fei Ding, Changhong Zhao,
Harsha Padullaparti, and Xin Jin

National Renewable Energy Laboratory

Suggested Citation
Utkarsh, Kumar, Fei Ding, Changhong Zhao, Harsha Padullaparti, and Xin Jin. 2020. *A Model-Predictive Hierarchical-Control Framework for Aggregating Residential DERs to Provide Grid Regulation Services: Preprint*. Golden, CO: National Renewable Energy Laboratory. NREL/CP-5D00-74827. https://www.nrel.gov/docs/fy20osti/74827.pdf.

NREL is a national laboratory of the U.S. Department of Energy
Office of Energy Efficiency & Renewable Energy
Operated by the Alliance for Sustainable Energy, LLC

This report is available at no cost from the National Renewable Energy Laboratory (NREL) at www.nrel.gov/publications.

Contract No. DE-AC36-08GO28308

Conference Paper
NREL/CP-5D00-74827
February 2020

National Renewable Energy Laboratory
15013 Denver West Parkway
Golden, CO 80401
303-275-3000 • www.nrel.gov

NOTICE

This work was authored by the National Renewable Energy Laboratory, operated by Alliance for Sustainable Energy, LLC, for the U.S. Department of Energy (DOE) under Contract No. DE-AC36-08GO28308. Funding provided by U.S. Department of Energy Office of Energy Efficiency and Renewable Energy Solar Energy Technologies Office. The views expressed herein do not necessarily represent the views of the DOE or the U.S. Government.

This report is available at no cost from the National Renewable Energy Laboratory (NREL) at www.nrel.gov/publications.

U.S. Department of Energy (DOE) reports produced after 1991 and a growing number of pre-1991 documents are available free via www.OSTI.gov.

Cover Photos by Dennis Schroeder: (clockwise, left to right) NREL 51934, NREL 45897, NREL 42160, NREL 45891, NREL 48097, NREL 46526.

NREL prints on paper that contains recycled content.

A Model-Predictive Hierarchical-Control Framework for Aggregating Residential DERs to Provide Grid Regulation Services

Kumar Utkarsh*, Fei Ding*, Changhong Zhao*, Harsha Padullaparti* and Xin Jin*
*National Renewable Energy Laboratory, 15013 Denver W Pkwy, Golden, CO, 80401
utkarsh.kumar@nrel.gov, fei.ding@nrel.gov

***Abstract*—This paper develops a hierarchical control framework to aggregate and to manage behind-the-meter distributed energy resources (DERs), which will be ubiquitous in future distribution systems. In the proposed framework, firstly, each controller in the hierarchy determines the flexibility of the DERs such that the obtained flexibility is *feasible* with respect to its operational purview. For example, the operational purview of a home energy management system may only consider consumer comfort preferences, while that for an aggregator or a grid controller may consider network voltage management as well. Based on the feasible flexibility, optimal setpoints for the DERs is then determined by the hierarchical controllers to help the distribution power network in voltage regulation, coordination issues with existing transmission-level conventional generators, etc. Therefore, the proposed strategy, which is based on model-predictive control, can be effectively utilized by the distribution network to coordinate several DERs to provide grid regulation services. Numerical simulations performed on the IEEE 37-bus test system demonstrate the efficacy of the proposed approach.**

Keywords—Flexibility, hierarchical control, model-predictive, distributed energy resource, behind-the-meter.

I. Introduction

The power system landscape is presently undergoing a dramatic change with the rapid integration of numerous distributed energy resources (DERs), mainly in medium- to low-voltage distribution networks. The increased adoption of distribution-level DERs will strain the distribution systems in terms of increased difficulty in network voltage regulation, increased power losses, and coordination issues with existing transmission-level conventional generators [1]. But distribution systems will also be able to provide a certain level of dispatchability or flexibility in their (re)active power in conjunction with DERs, such as electric water heaters (EWHs) and energy storage systems (ESSs). This will ensure that distribution systems will be able to participate in grid regulation services by aggregating several DERs, thereby providing cost savings to the DER owners[2]-[3].

Several researchers have focused on controlling distribution system DERs by considering their aggregated flexibility. Flexibility can be characterized in terms of the set of all the power trajectories that a DER can have, and the strategies developed to obtain flexibility can be divided into three main categories—power nodes [4]—[5], generalized batteries [6]—[7], and resource polytopes [8]—[10]. The flexibility thus obtained of each DER can then be aggregated to obtain the net flexibility of the distribution system. Most studies, however, do not consider the constraints of the distribution power network itself when calculating the aggregated distribution system flexibility. Thus, the optimal solution obtained for DER setpoints considering DER flexibility might not be feasible with respect to the distribution power system.

Therefore, in this paper, we first identify the flexibility of each DER considering behind-the-meter DER owners' (customers') comfort requirements based on model-predictive control. This flexibility information is then sent to an *Aggregator*, which aggregates the information sent by the DER owners and identifies the net flexibility information for the distribution network under its purview while considering unbalanced power flow solution and network voltage constraints. This enables small-scale DERs to participate in grid services and gain economic benefits. The main contributions of this paper are as follows:

1) A model-predictive strategy is proposed to determine the flexibility as well as the preferred setpoints of the DERs based on a convex optimization model.

2) An aggregation and a disaggregation strategy are proposed considering the unbalanced power flows in distribution systems and their network constraints.

The rest of this paper is organized as follows. Section II presents the envisioned information and control flow; sections III and IV present models for the home energy management system (HEMS) and the Aggregator, respectively; section V presents simulation results; and section VI concludes.

II. Information and Control Flow

Fig. 1 depicts the envisioned architecture and it is assumed that the distribution network is divided into several communities, each of which is controlled by an Aggregator. In this paper, we focus on developing the control strategy for a single community, and this strategy can be easily extended to multiple communities. Each community consists of multiple smart homes, and each home is assumed to be managed by a HEMS, which gathers information from and controls the set-points of the DERs present in that home. The HEMS of all the homes also share information with the Aggregator, which determines suitable set-points for each HEMS by considering the network power flow and its constraints.

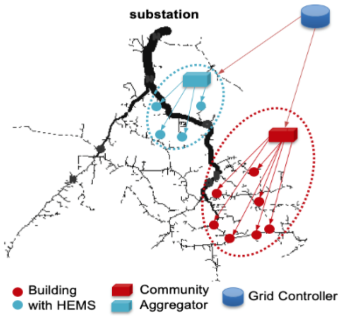

Fig. 1. A general representation of the power system architecture.

The overall information and control flow *for each time step* of a certain duration can be summarized as follows:

***Step 1*: HEMS Optimization A**: The HEMS for each smart home takes information from the DERs and other uncontrollable loads in the home. It then solves an optimization problem to determine the feasible set of DER powers such that they always satisfy the bounds of comfort requirements set by the homeowner. This feasible set consists of the feasible power bounds and the nominal power corresponding to maximum cost efficiency. Such feasible power bounds and the nominal power for each home are then sent to the Aggregator.

***Step 2*: Aggregator Optimization A**: The power bounds and the nominal power received from each HEMS are fed to an optimization framework in the Aggregator so that their feasibility with respect to the power network as well can be determined. The Aggregator solves this optimization considering the power network constraints, the nominal power sent by each HEMS, and the grid service requests, and it outputs a feasible power bound at the point of common coupling (PCC) along with a nominal PCC power to be sent to the grid controller so that the aggregated DERs can participate in the grid services market. Note that the grid controller and how the grid services market is cleared are not handled by this work.

***Step 3*: Aggregator Optimization B**: Once the grid controller clears the market, it sends power request signals to the Aggregator to be maintained at the PCC. The Aggregator then performs an economic disaggregation optimization such that the grid power request signals are tracked closely in an efficient manner, and it outputs the power setpoints for each HEMS.

***Step 4*: HEMS Optimization B**: Like the Aggregator disaggregation algorithm, the HEMS of each smart home performs a disaggregation optimization of the setpoints given by Aggregator Optimization B, and it outputs the setpoints to be implemented by each DER.

The proposed control strategy is based on the development of convex optimization models for *(i)* a HEMS, which manages various DERs in a smart home, and *(ii)* an Aggregator, which coordinates multiple homes in a community subnetwork and fulfills grid service requests from the grid controller. The optimization models for the HEMSs and the Aggregator are elaborated in the following sections.

III. Home Energy Management System

A. DER Models

For ease of exposition, we consider a representative case where every home has PV; a battery ESS; a heating, ventilating, and air conditioning (HVAC) appliance; an EWH; and an aggregated uncontrollable load (aggregated lighting, television, plug loads, etc.). In this section, we use i to index homes and t to index time slots at which power dispatch is carried out. Typically, each time slot is assumed as 15 mins. The models for individual DERs are presented next (see [11], [12] for details).

1) The PV unit can be modeled as*:*

$$0 \le p_{i,pv}^t \le \overline{p}_{i,pv}^t \quad ; \quad \left(p_{i,pv}^t\right)^2 + \left(q_{i,pv}^t\right)^2 \le \left(\overline{s}_{i,pv}\right)^2$$
$$q_{i,pv}^t \le \overline{\gamma}_{i,pv} p_{i,pv}^t \quad ; \quad q_{i,pv}^t \ge -\overline{\gamma}_{i,pv} p_{i,pv}^t \qquad \forall i, \forall t \qquad (1)$$

where $p_{i,pv}^t$ and $q_{i,pv}^t$ are (re)active power injections; $\overline{p}_{i,pv}^t$ is the maximum available PV active power injection; $\overline{s}_{i,pv}$ is the rating of the PV unit; and $\overline{\gamma}_{i,pv}$ limits the operating power factor—in other words, $1/\sqrt{1+\overline{\gamma}_{i,pv}^2}$ is the minimum power factor allowed for this PV unit, in both leading and lagging directions.

2) The battery state of charge, B_i^t, is modeled based on [11], with the following additions for reactive power control:

$$q_{i,c}^t \ge -\overline{\gamma}_{i,c}\, p_{i,c}^t \quad ; \quad q_{i,d}^t \le \overline{\gamma}_{i,d}\, p_{i,d}^t$$
$$\left(q_{i,d}^t - q_{i,c}^t\right)^2 + \left(p_{i,d}^t - p_{i,c}^t\right)^2 \le \left(\overline{s}_{i,b}\right)^2 \qquad \forall i, \forall t \ (2)$$

where $p_{i,c}^t$, $p_{i,d}^t$, $q_{i,c}^t$ and $q_{i,d}^t$ are the active/reactive charging and discharging power; and the constants $\overline{\gamma}_{i,c}$ and $\overline{\gamma}_{i,d}$ limit the operating power factor of the battery.

3) The HVAC system is modeled based on [11], with the following additions for reactive power control:

$$q_{i,hvac}^t = \overline{\gamma}_{i,hvac}\left(I_{i,ht}^t \overline{p}_{i,ht} + I_{i,cl}^t \overline{p}_{i,cl}\right) \qquad \forall i, \forall t \ (3)$$

where $I_{i,ht}^t$ and $I_{i,cl}^t$ are the heating and cooling control signals in duty-cycle forms; $\overline{p}_{i,ht}$ and $\overline{p}_{i,cl}$ are delivered maximum heating and cooling power; and $\overline{\gamma}_{i,hvac}$ indicates constant power factor $1/\sqrt{1+\overline{\gamma}_{i,hvac}^2}$.

4) The water heater is modeled based on [11], with the following additions for reactive power control*:*

$$q_{i,wh}^t = \overline{\gamma}_{i,wh}\left(I_{i,low}^t + I_{i,up}^t\right) \overline{p}_{i,wh} \qquad \forall i, \forall t \ \ (4)$$

where $I_{i,low}^t, I_{i,up}^t$ are duty cycles (control decisions) of the lower and upper nodes of the heater; $\overline{p}_{i,wh}$ is the delivered maximum power; $q_{i,wh}^t$ is the reactive power load; and $\overline{\gamma}_{i,wh}$ indicates constant power factor $1/\sqrt{1+\overline{\gamma}_{i,wh}^2}$.

B. HEMS Optimization A

With these DER models, we get the net active and reactive power consumptions of home i at time t:

$$p_i^t = -p_{i,pv}^t + \left(p_{i,c}^t - p_{i,d}^t\right) + \left(I_{i,ht}^t \overline{p}_{i,ht} + I_{i,cl}^t \overline{p}_{i,cl}\right) + \left(I_{i,low}^t + I_{i,up}^t\right) \overline{p}_{i,wh} + p_{i,l}^t \qquad (5a)$$
$$q_i^t = -q_{i,pv}^t + \left(q_{i,c}^t - q_{i,d}^t\right) + q_{i,hvac}^t + q_{i,wh}^t + q_{i,l}^t \qquad (5b)$$

where $p_{i,l}^t$ and $q_{i,l}^t$ are the aggregate active and reactive power consumption of uncontrollable loads. For convenience, we denote the vector of all the control and state variables at home i at time t as z_i^t.

At time t_s, given the predictions and aggregate active and reactive power consumptions of uncontrollable loads over $t = \{t_s, t_s + 1 \ldots, t_s + T - 1\}$, every HEMS i (which manages home i) calculates a trajectory of upper bound $(p_{i,\wedge}^t, q_{i,\wedge}^t)$ and lower bound $(p_{i,\vee}^t, q_{i,\vee}^t)$ for its net active and reactive power consumptions. These two trajectories define the flexibility of home i in providing active and reactive power regulation services to the grid. In addition, a nominal/preferred trajectory $z_{i,o}^t$ is determined that aims to maximize economic efficiency and the user comfort level of home i. All three trajectories can be solved together using the following optimization problem:

$$\max\Big[\min_t \{b_{i,flex,p}^t\left(p_{i,\wedge}^t - p_{i,\vee}^t\right) + \min_t b_{i,flex,q}^t\left(q_{i,\wedge}^t - q_{i,\vee}^t\right)\} - \sum_t \left(b_{i,p}^t p_{i,o}^t + b_{i,q}^t q_{i,o}^t + b_{i,c}^t p_{i,c,o}^t + b_{i,d}^t p_{i,d,o}^t\right) - b_{i,hvac}^t\left(T_{i,in,o}^t - T_{i,in,ref}^t\right)^2 - b_{i,wh}^t\left(T_{i,up,o}^t - T_{i,up,ref}^t\right)^2\Big] \quad (6a)$$

$$over \quad z_{i,\wedge}^t, z_{i,\vee}^t, z_{i,o}^t, \forall t$$

$$subject\ to \ \ (1)-(5)\ for\ z_{i,\wedge}^t, z_{i,\vee}^t, z_{i,o}^t \ \ \forall t \qquad (6b)$$

$$p_{i,\wedge}^t \ge p_{i,o}^t \ge p_{i,\vee}^t, q_{i,\wedge}^t \ge q_{i,o}^t \ge q_{i,\vee}^t, \forall t \qquad (6c)$$

The objective function (6a) rewards the flexibility of home i in its net active and reactive power consumptions, measured by the weighted sum (with weighting factors $b_{i,flex,p}^{t}$ and $b_{i,flex,q}^{t}$). Also, $b_{i,p}^{t}p_{i,o}^{t}$ and $b_{i,q}^{t}q_{i,o}^{t}$ are the costs for net active and reactive power consumptions of home i, respectively; and $b_{i,c}^{t}\, p_{i,c,o}^{t}$ and $b_{i,d}^{t}p_{i,d,o}^{t}$ are the costs associated with battery charging and discharging, e.g., for battery life reduction. The last two terms in (6a) penalize deviations of indoor air temperature and upper-node water temperature from their preset reference values, or user-preferred values, $T_{i,in,ref}^{t}$ and $T_{i,up,ref}^{t}$. The constraints ensure the feasibility of DER operating points in upper, lower, and nominal cases.

C. HEMS Optimization B

After each HEMS receives the setpoints from the Aggregator at Step 4, it performs an economic disaggregation optimization to determine the setpoints of its DERs. For the time-step t_s, this disaggregation is performed using the following optimization problem:

$$\min \sum_{t} \left[\beta_{i,p}^{t}\left(p_{i,d,*}^{t} - p_{i,d,o}^{t}\right)^2 + \beta_{i,q}^{t}\left(q_{i,d,*}^{t} - q_{i,d,o}^{t}\right)^2\right] \quad (7a)$$

$$\textit{subject to} \quad 0 < \varepsilon \ll 1 \;;\; (1)-(5)\; for\; z_{i,d,*}^{t}, \forall t \quad (7b)$$

$$p_{i,agg}^{t} - \varepsilon \le \sum_{d}\left[p_{i,d,*}^{t}\right] \le p_{i,agg}^{t} + \varepsilon, \;\; \forall t \quad (7c)$$

$$q_{i,agg}^{t} - \varepsilon \le \sum_{d}\left[q_{i,d,*}^{t}\right] \le q_{i,agg}^{t} + \varepsilon, \;\; \forall t \quad (7d)$$

where the subscript *d* denotes power for the DER *d* controlled by HEMS i, and (*) represents the final optimal value to be implemented by the DER *d*.

IV. Aggregator

The Aggregator of a community manages the smart homes in that community while considering network constraints, and acts as a cyber interface between the HEMS and the grid controller, thereby enabling the home DERs to participate in the grid services markets. The network constraints are handled by using a linearized unbalanced power flow model of the distribution network.

A. Linear Power-Flow Model of the Distribution Network

We use $i \in N$ to index multiphase buses in the considered network. Assume that the considered network has only one PCC with the upstream network, and let the PCC be indexed as bus $0 \in N$. Let the set of non-PCC buses be denoted as $N^{+} := N\backslash\{0\}$, and let a, b, c denote the three phases, and Φ_i the set of phases of bus i. Denote by $v := \left[v_i^{\phi}, \phi \in \Phi_i, i \in N^{+}\right]$, $p := [p_i^{\phi}, \phi \in \Phi_i, i \in N^{+}]$, $q := [q_i^{\phi}, \phi \in \Phi_i, i \in N^{+}]$ the vectors of the squared voltage magnitudes and of the active and reactive power consumptions, respectively, at all the phases of all the non-PCC buses. With this notation, we use a linearized distribution power flow model [13] for the multiphase unbalanced distribution network as shown in (8a), where vector $\tilde{v}_0 := [v_0^{\phi}]$ collects squared voltage magnitudes at different phases of the PCC bus. The elements of the matrices R and X are defined in (8b)-(8d) ($a = 0, b = 1, c = 2$ are used to calculate phase differences):

$$v = Rp + Xq + \tilde{v}_0 \quad (8a)$$

$$\partial_{p_j^{\phi}} v_i^{\psi} = -2Re\left\{\overline{Z}_{ij}^{\psi\phi} e^{-\frac{i2\pi(\psi-\phi)}{3}}\right\} \quad (8b)$$

$$\partial_{q_j^{\phi}} v_i^{\psi} = +2Im\left\{\overline{Z}_{ij}^{\psi\phi} e^{-\frac{i2\pi(\psi-\phi)}{3}}\right\} \quad (8c)$$

where $\bar{\cdot}$ denotes complex conjugate, and

$$Z_{ij}^{\psi\phi} := \sum_{(\xi,\zeta)\in E_i \cap E_j} z_{\xi\zeta}^{\psi\phi} \quad (8d)$$

B. Aggregator Optimization A

After the Aggregator receives the power bounds and nominal power from each HEMS at time t_s, it performs an optimization to determine the feasible bounds and nominal power at the PCC considering the power network constraints using the optimization problem developed here.

The active and reactive power flows at the PCC are:

$$p_0^{\phi} = \sum_{i\in N^{+}} p_i^{\phi}, \forall \phi \in \Phi_0 \;\; ; \;\; q_0^{\phi} = \sum_{i\in N^{+}} q_i^{\phi}, \forall \phi \in \Phi_0 \quad (9)$$

The Aggregator also receives grid service commands $(p_{0,comm}^{\phi,t}, q_{0,comm}^{\phi,t}, \phi \in \Phi_0)$ over $t = \{t_s, t_s + 1 \ldots, t_s + T - 1\}$, which are the net active and reactive power consumptions of the considered network. The following optimization aims to solve for the upper trajectory $(p_{0,\wedge*}^{t}, q_{0,\wedge*}^{t})$ and lower trajectory $(p_{0,\vee*}^{t}, q_{0,\vee*}^{t})$ for the net power consumption at the PCC as well as the nominal dispatch decisions $(p_{i,*}^{\phi,t}, q_{i,*}^{\phi,t}, \phi \in \Phi_i, i \in N^{+})$:

$$\min \sum_{t}\sum_{i\in N^{+}}\sum_{\phi\in\Phi_i}\left[\gamma_{i,p}^{\phi,t}\left(p_{i,*}^{\phi,t} - p_{i,o}^{\phi,t}\right)^2 + \gamma_{i,q}^{\phi,t}\left(q_{i,*}^{\phi,t} - q_{i,o}^{\phi,t}\right)^2\right]$$
$$+ \sum_{\phi\in\Phi_0}\left[\gamma_{0,p}^{\phi,t}\left(p_{0,*}^{\phi,t} - p_{0,comm}^{\phi,t}\right)^2 + \gamma_{0,q}^{\phi,t}\left(q_{0,*}^{\phi,t} - q_{0,comm}^{\phi,t}\right)^2\right]$$
$$-\sum_{t}\sum_{\phi\in\Phi_i}\left[\gamma_{0,flex,p}^{\phi,t}\min_{t}\left(p_{0,\wedge*}^{\phi,t} - p_{0,\vee*}^{\phi,t}\right)\right.$$
$$\left. + \gamma_{0,flex,q}^{\phi,t}\min_{t}\left(q_{0,\wedge*}^{\phi,t} - q_{0,\vee*}^{\phi,t}\right)\right] \quad (10a)$$

$$\textit{over} \quad v_*^t, p_*^t, q_*^t, v_{0,*}^t, p_{0,*}^t, q_{0,*}^t, v_{\wedge*}^t, p_{\wedge*}^t, q_{\wedge*}^t, v_{0,\wedge*}^t, p_{0,\wedge*}^t, q_{0,\wedge*}^t, v_{\vee*}^t, p_{\vee*}^t, q_{\vee*}^t, v_{0,\vee*}^t, p_{0,\vee*}^t, q_{0,\vee*}^t, \forall t$$

$$\textit{subject to} \;\; (8)-(9)\; for\; v_*^t, p_*^t, q_*^t, v_{0,*}^t, p_{0,*}^t, q_{0,*}^t, \forall t \quad (10b)$$

$$(8)-(9)\; for\; v_{\wedge*}^t, p_{\wedge*}^t, q_{\wedge*}^t, v_{0,\wedge*}^t, p_{0,\wedge*}^t, q_{0,\wedge*}^t, \forall t \quad (10c)$$

$$(8)-(9)\; for\; v_{\vee*}^t, p_{\vee*}^t, q_{\vee*}^t, v_{0,\vee*}^t, p_{0,\vee*}^t, q_{0,\vee*}^t, \forall t \quad (10d)$$

$$p_{\vee}^t \le p_*^t \le p_{\wedge}^t, \quad q_{\vee}^t \le q_*^t \le q_{\wedge}^t, \forall t \quad (10e)$$

$$p_{\vee}^t \le p_{\wedge*}^t \le p_{\wedge}^t, \quad q_{\vee}^t \le q_{\wedge*}^t \le q_{\wedge}^t, \forall t \quad (10f)$$

$$p_{\vee}^t \le p_{\vee*}^t \le p_{\wedge}^t, \quad q_{\vee}^t \le q_{\vee*}^t \le q_{\wedge}^t, \forall t \quad (10g)$$

$$\underline{v} \le v_*^t \le \overline{v}, \quad \underline{v}_0 \le v_{0,*}^t \le \overline{v}_0, \forall t \quad (10h)$$

$$\underline{v} \le v_{\wedge*}^t \le \overline{v}, \quad \underline{v}_0 \le v_{0,\wedge*}^t \le \overline{v}_0, \forall t \quad (10i)$$

$$\underline{v} \le v_{\vee*}^t \le \overline{v}, \quad \underline{v}_0 \le v_{0,\vee*}^t \le \overline{v}_0, \forall t \quad (10j)$$

$$p_{0,\vee*}^t \le p_{0,*}^t \le p_{0,\wedge*}^t, \quad q_{0,\vee*}^t \le q_{0,*}^t \le q_{0,\wedge*}^t, \forall t \quad (10k)$$

The objective (10a) aims to minimize the deviation of the power dispatch commands from their nominal/preferred values submitted by the HEMS as well as the deviation of the resulting net power consumptions at the PCC from the grid service requests $(p_{0,comm}^{t}, q_{0,comm}^{t})$. It also rewards the flexibility of the net active and reactive power consumption at the PCC. The constraints ensure feasibility in terms of network power flow, and available power bounds of HEMS.

C. Aggregator Optimization B

Once the grid controller clears the market, it sends request signals for active/reactive power to the Aggregator to be maintained at the PCC. The Aggregator then performs an economic disaggregation optimization using the following optimization problem and sends the signals $p_{i,agg}^{t}$ and $q_{i,agg}^{t}$ to each HEMS i for tracking.

$$\min \sum_t \left\{ \sum_{i\in N^+} \sum_{\phi\in\Phi_i} \left[\gamma_{i,p}^{\phi,t} \left(p_{i,agg}^{t} - p_{i,o}^{\phi,t} \right)^2 + \gamma_{i,q}^{\phi,t} \left(q_{i,agg}^{t} - q_{i,o}^{\phi,t} \right)^2 \right] \right\} \quad (11a)$$

$$\textit{subject to} \qquad 0 < \varepsilon \ll 1 \;\; ; \;\; (8) - (9)\,, \qquad \forall t \qquad (11b)$$

$$p_{0,comm}^{\phi,t} - \varepsilon \le \sum_i \left[p_{i,agg}^{t} \right] \le p_{0,comm}^{\phi,t} + \varepsilon, \;\; \forall t \quad (11c)$$

$$q_{0,comm}^{\phi,t} - \varepsilon \le \sum_i \left[q_{i,agg}^{t} \right] \le q_{0,comm}^{\phi,t} + \varepsilon, \;\; \forall t \quad (11d)$$

V. Simulation Results and Discussion

Numerical tests of the proposed control strategy are performed on an IEEE 37-bus test system, which is a three-phase distribution test feeder widely used for numerical simulations. The optimization solver ECOS [14] with error tolerance of 1e-6 was used to solve the convex optimization models presented in Section-IV. It is assumed that the entire 37-bus system is a single community and is controlled by a single Aggregator. Further, each node (each of the three phases of each bus) is assumed to be a smart home managed by a HEMS.

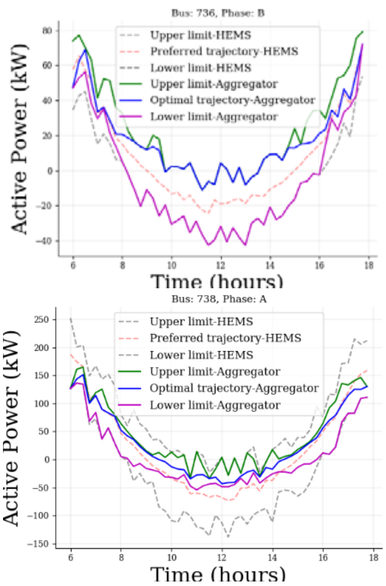

Fig. 2. Power profiles for two HEMS.

To demonstrate the effectiveness of the proposed control strategy, first, at the beginning of each time step *Ts=15 min*, the upper ($p_{i,\wedge}^t, q_{i,\wedge}^t$) and lower bounds ($p_{i,\vee}^t, q_{i,\vee}^t$) and nominal power ($p_{i,0}^t, q_{i,0}^t$) are obtained by each HEMS i using *HEMS Optimization A* based on arbitrary but realistic parameter values for the DERs (Step 1). These bounds and nominal power are calculated and shown for two representative HEMS at two nodes—Bus 736 Phase B and Bus 738 Phase A—in Fig. 2 using dashed lines for a 12-hour duration from 6 a.m. to 6 p.m. These two nodes are chosen such that they are representative of both ends of the load spectrum: Bus 736 Phase B belongs to the set of nodes with the lowest net-loads, and Bus 738 Phase A belongs to the set of nodes with the highest net loads. Fig. 2 shows that the flexible bands for both nodes (dashed lines) are quite uniform in width throughout the time horizon because each HEMS considers only their comfort requirements and not the power network constraints in Step 1.

These bounds and nominal powers from the HEMSs are then sent to the Aggregator, which performs its own optimization using *Aggregator Optimization A* to determine the new feasible bounds and nominal power based on unbalanced power flows and network voltage constraints of $\pm$ 5%. The new *network-feasible* power bounds obtained by the Aggregator are shown in Fig. 2 for the two nodes using green and magenta solid lines. As shown in Fig. 2, for both nodes, the new power bounds obtained by the Aggregator might not overlap exactly with those provided by the HEMS; instead, they are usually narrower. It is noticed that the feasible band provided by the Aggregator for Bus 736 Phase B is similar to that provided by the HEMS at that node. On the other hand, the feasible band provided by the Aggregator for Bus 738 Phase A is much narrower than that provided by the HEMS at that node. This is because Bus 738 has a much higher net load compared to Bus 736, and the Aggregator optimizes them such that there are no voltage violations along with other constraints as in (10). This is also visible in Fig. 3, which shows the minimum and maximum voltages at the nodes to be inside the chosen limit of $\pm$ 5% for the optimal, upper and lower trajectories provided by the Aggregator.

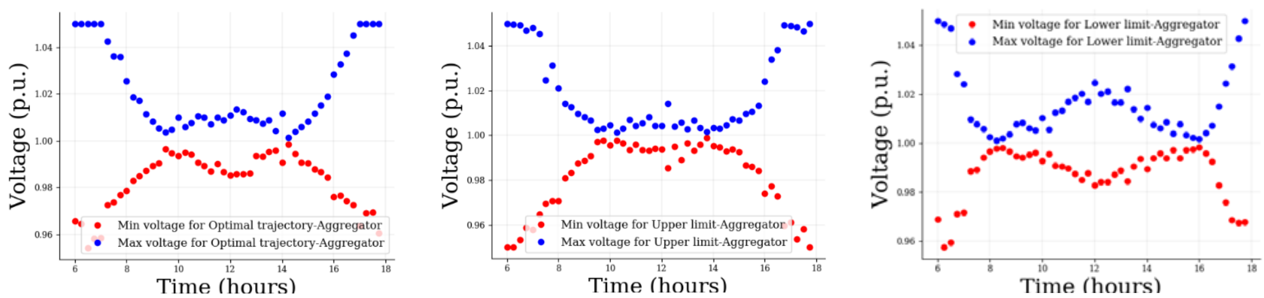

Fig. 3. Node voltages corresponding to the Aggregator's *1)* optimal trajectory, *2)* upper limit trajectory, and *3)* lower limit trajectory.

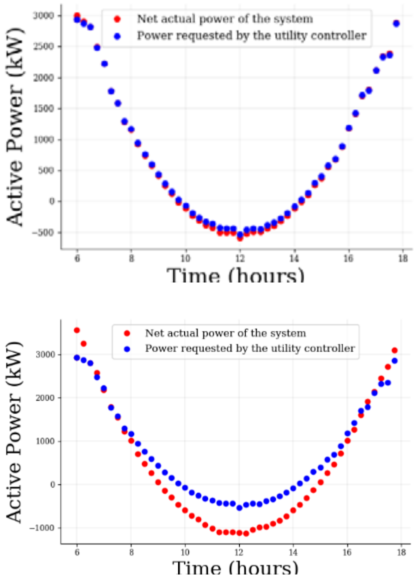

Fig. 4. Net power profiles at the PCC.

Further, the weight factors γ can be tuned to make the Aggregator prefer the trajectories given by the HEMS more closely than the trajectory requested by the grid controller, or vice versa. Fig. 4 shows the preferred power dispatch of the Aggregator compared to that requested by the grid controller, for two different sets of weight factors. When the weight factors $\gamma_{0,p}^{\phi,t}$ and $\gamma_{0,q}^{\phi,t}$ are reduced, the preferred dispatch trajectory of the Aggregator deviates away from the grid-requested trajectory while deviating toward the trajectory preferred by HEMS, as shown in Fig. 5.

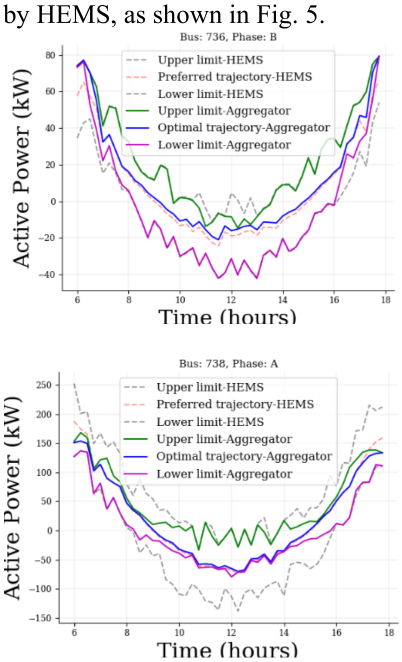

Fig. 5. Power profiles for two HEMS for different weights.

The next step involves the Aggregator transmitting the PCC feasible flexibility information along with nominal power to the grid controller, which then clears the market and gives $p_{0,comm}^{\phi,t}$ and $q_{0,comm}^{\phi,t}$ to be tracked by the Aggregator at the community PCC. Therefore, the Aggregator performs *Aggregator Optimization B* to economically disaggregate the grid request signals to be sent to each HEMS. These are shown as blue solid lines for the two nodes in Fig. 2. Finally, each HEMS performs *HEMS Optimization B* to disaggregate the Aggregator signal to be sent to each DER for set-point implementation. It is noted that the combined simulation runtime for HEMS as well as Aggregator Optimizations A and B was less than 8 seconds for a Python implementation running on a 4 GHz Intel processor.

VI. Conclusions and Future Work

This paper introduced a hierarchical control framework to determine the available power flexibility of the smart homes in a distribution system as well as of the distribution system itself, considering unbalanced power flow formulation and network voltage constraints. The bi-directional flow of information and control ensures that the distribution-level DERs are also able to participate in the grid services markets, thereby helping the power network use the DER flexibility while earning cost savings for the DER owner. Simulation studies performed on the IEEE 37-bus test system showed that the proposed approach can be effectively used for coordination of distribution-system DERs with the upstream power network while taking full consideration of the distribution system topology and constraints.

The proposed framework is well suited to accommodate other DER types, such as electric vehicles, as well as cost benefit maximization of individual controllers in the hierarchy, which will be studied extensively in our future work.

Acknowledgment

This work was authored by the National Renewable Energy Laboratory, operated by Alliance for Sustainable Energy, LLC, for the U.S. Department of Energy (DOE) under Contract No. DE-AC36-08GO28308. Funding provided by the U.S. DOE Office of Energy Efficiency and Renewable Energy Solar Energy Technologies Office. The views expressed in the article do not necessarily represent the views of the DOE or the U.S. Government. The U.S. Government retains and the publisher, by accepting the article for publication, acknowledges that the U.S. Government retains a nonexclusive, paid-up, irrevocable, worldwide license to publish or reproduce the published form of this work or allow others to do so, for U.S. Government purposes.

References

[1] M. Yazdanian and A. Mehrizi-Sani, "Distributed Control Techniques in Microgrids," *IEEE Transactions on Smart Grid,* vol. 5, no. 6, pp. 2901-2909, 2014.

[2] H. Sun, Q. Guo, B. Zhang, Y. Guo, Z. Li, and J. Wang, "Masterslave splitting based distributed global power flow method for integrated transmission and distribution analysis," IEEE Trans. Smart Grid, vol. 6, no. 3, pp. 1484-1492, May.

[3] C. D'Adamo, S. Jupe, and C. Abbey, "Global survey on planning and operation of active distribution networks-Update of CIGRE C6.11working group activities," in Proc. 20th Int. Conf. Exhibit. Elect. Distrib.,Prague, Czech Republic, 2009.

[4] A. Ulbig and G. Andersson, "On Operational Flexibility in Power Systems," in *IEEE Power and Energy Soc. Gen. Meeting*, IEEE, 2012, pp. 1–8

[5] S. Koch and G. Andersson, "Assessment of Revenue Potentials of Ancillary Service Provision by Flexible Unit Portfolios," in *IEEE Power and Energy Soc. General Meeting*. IEEE, 2012, pp. 1–8.

[6] A. Nayyar, J. Taylor, A. Subramanian, K. Poolla, and P. Varaiya, "Aggregate Flexibility of a Collection of Loads," in *52nd IEEE Conf. Decision and Control*. IEEE, 2013, pp. 5600–5607.

[7] H. Hao, B. M. Sanandaji, K. Poolla, and T. L. Vincent, "A Generalized Battery Model of a Collection of Thermostatically Controlled Loads for Providing Ancillary Service," in *51st Allerton Conf. on Communication, Control, and Computing*. IEEE, 2013, pp. 551–558.

[8] K. Trangbaek and J. Bendtsen, "Exact Constraint Aggregation with Applications to Smart Grids and Resource Distribution," in *51st IEEE Conf. Decision and Control*. IEEE, 2012, pp. 4181–4186.

[9] L. Zhao, H. Hao, and W. Zhang, "Extracting Flexibility of Heterogeneous Deferrable Loads via Polytopic Projection Approximation," in *55th IEEE Conf. Decision and Control*. IEEE, 2016, pp. 6651–6656.

[10] F. L. Muller, O. Sundstrom, J. Szabo, and J. Lygeros, "Aggregation of Energetic Flexibility Using Zonotopes," in *54th IEEE Conf. Decision and Contro*l. IEEE, 2015, pp. 6564–6569.

[11] X. Jin, K. Baker, S. Isley, and D. Christensen, "User-preference-driven model predictive control of residential building loads and battery storage for demand response," *American Control Conference*, Seattle, WA, USA, May 2017, pp. 4147—4152.

[12] X. Jin, K. Baker, D. Christensen, and S. Isley, "Foresee: A user-centric home energy management system for energy efficiency and demand response," *Applied Energy*, no. 205, pp. 1583—1595, November 2017.

[13] L. Gan and S. H. Low, "Convex relaxations and linear approximation for optimal power flow in multiphase radial networks," *Power Systems Computation Conference*, Wroclaw, Poland, 2014.

[14] https://web.stanford.edu/~boyd/papers/ecos.html